OPTIMIZATION DESIGN OF CARBON FIBER LAYOUT IN COMPOSITE STRUCTURES WITH X-SHAPED JUNCTION BASED ON FINITE ELEMENT SIMULATION

J. Y. Liu[1, 2], W. D. Chen[1], D. Z. Jiang[1*]

[1] Shenzhen Campus of Sun Yat-sen University 518107, P.R. China; jiangdzhi@mail.sysu.edu.cn
[2] Synchrotron radiation facility, Institute of advanced science facilities, Guangming, Shenzhen, Guangdong, 518107, People's Republic of China

Keywords: carbon fiber reinforced composite materials; lattice structure; cross ribs; thin-ply; finite element simulation

ABSTRACT

Nowadays, carbon fiber reinforced polymer matrix composite materials are widely used in truss and lattice structures for their light weight and high mechanical properties. However, the nature of the cross junction of the fibers in ribs of the structures decreased the load capability. To solve this problem, an example of X-shaped structure design is presented in this paper. A local thin-ply technology is applied to achieve carbon fiber layout, which aims at making full use of the axial advantage of the carbon fibers. The finite element simulation methods are applied to assist the carbon fiber layout design. In the simulation, inverse homogeneity transformation and dehomogeneity transformation are realized through the Swift-comp software to establish the relation between macro and micro structures according to the structural gene theory. The advantages of the local thin-ply structure are verified, compared with the traditional structure, the stiffness is increased by 4%-27% and the maximum stress at the intersection point is decreased by 28%-60%. The optimum width-thickness ratio of local thin-ply is determined to be 80/0.15. A broadly applicable composite structure design scheme is finally obtained, which will provide reference for future engineering progress.

1 INTRODUCTION

With rapid development of spacecraft and aircraft engineering, requirements for materials in those fields are getting higher[1-5]. Lighter and stronger materials are needed. Composite material has the characteristic of anisotropy, which makes it more suitable for one-way bearing structures such as truss and lattice[6-8]. Spacecrafts often use these structures, the design of which is one of the core technologies for aerospace development. Researches have been carried out to explore and verify the reliability for composite materials acting as load-bearing parts[9-12].

At present, composites have been widely adopted in the aerospace field, such as the spacecraft fuselage, helicopter tail and rocket bearing barrel[13-15]. US Air Force Laboratory applied carbon fiber reinforced polymer matrix composites (CFRP) in the AGS fairing to strengthen the ribs forming a lattice structure[16, 17]. The automatic production was achieved through fiber winding technology, which greatly shortened the production process. Compared with similar products at that time, 40% of the overall weight loss and 20% of the cost reduction were both achieved. The technology was later further promoted by the United States Air Force.

NASA has designed a spindle-type hollow(tube) support rod using composite truss unit structure[18, 19], which had been successfully applied in the lunar lander by 2009. At present, it has attracted extensive attention. Northrop and Boeing used IM7-977-3/IM7-8552 carbon fiber and epoxy resin to produce heavy-duty spindle-shaped composite tubes and lightweight spindle-shaped composite tubes, respectively.

For continuous fiber composite lattice, truss and other similar structures, intersection of the ribs is inevitable[20]. The cross position brings difficulties to the structural design process, carbon fiber orientation can hardly meet the load bearing demand in different directions at the same time. The conventional methods to handle this include direct stacking and carbon fabric cutting[21, 22]. The former leads to local uplift of macrostructure and stress concentration. Although the latter avoids this problem, the cutting process lowers fiber continuity and the orthotropic ply orientation attenuates its anisotropy advantage. Neither can make full use of the axial bearing capacity of carbon fiber. Actually, even for the simplest rib structure, due to the operation precision, there will be a slight deviation between the fiber orientation and the stress direction. Therefore, problems of the carbon fiber distribution optimization are generally presented in composite structures[23, 24]. So far, research on this aspect is still in a blank stage. It is necessary to put forward an applicable carbon fiber layout design method through exploration.

This paper aims to meet the requirements of high efficiency load-bearing structures in the aerospace field, propose a structural optimization method that can give full play to the axial load-bearing advantages of continuous fibers in composite laminating. Taking an X-type structure for example, the local thin-ply technology is introduced in the cross section, which can widen and thin the ply by reasonable arrangement of carbon fiber to avoid local thickening and fiber bulge[25, 26]. The corresponding relationship between the carbon fiber orientation and properties of the composite structures is investigated, a reliable scheme to improve the load-bearing properties is presented.

2. MATERIALS AND METHODS

In order to study the relationships between the carbon fiber distribution in micro-scale and the bearing capacity of macro structure, cross-scale modeling technique is required[27, 28]. The traditional idea is to find out the average performance parameters by homogenization of the micro-structure, treat the macro model as homogeneous material using the homogenized parameter. The homogenization method applied in this process is irreversible, thus it is impossible to reflect the relationship between the micro structure and the macro performance.

This paper intends to realize the transformation between the macro-micro models by introducing the structural gene theory[29, 30]. The specific operation is implemented through Swift-comp software®, which can establish a micro-representative unit according to the actual distribution of carbon fiber, and realize the structural homogenization transformation to obtain the average performance parameters. Different from the traditional method, this process is completed by analytic transformation under the premise of ensuring the lowest overall energy change of the structure, which is reversible (dehomogenization is realizable) and more accurate. The macro model is established by Abaqus software and the homogenized parameters are brought into the simulation to get the stress and strain distribution on the macro-scale. Then, the strain states of the concerned position are brought back to the representative micro-unit as boundary conditions to realize the structural dehomogenization by analytical inverse transformation to obtain the information on the micro scale. Thus, the correspondence relation between the micro-structure and the macro mechanical properties is established. The material parameters used in the simulation are shown in Table 1.

Table 1. parameters of carbon fiber and resin matrix[35]

Property	Value
E1 for carbon fiber	230GPa
E2=E3 for carbon fiber	12GPa
G12=G13=G23 for carbon fiber	5GPa
N Poisson for carbon fiber	0.3
E for epoxy resin matrix	3GPa
N Poisson for epoxy resin matrix	0.3

3 RESULTS AND DISCUSSION

3.1 Structural Design

3.1.1 Macro-scale model simplification

The cross-scale structure design needs to consider both the micro-structure and the macro-performance, which brings challenges to the calculation ability. While, the commonly used macro composite rib system such as truss and lattice structures contain a great number of rib members, directly cross scale modeling is not desirable. Reasonable simplification is necessary, the actual engineering components can be converted into abstract theoretical models.

Taking the commonly used connection bracket as an example, shown in Fig.1. The lattice structure is composed of a certain amount of composite ribs, the ribs intersect with each other to improve the overall stability. It is found that the whole structure is formed by a periodic arrangement of X-shaped units. For the rotational symmetry, each X-shaped structure has similar stress states. Thus, the macro structure is simplified and one of the X units can be taken out for analysis to improve the calculation efficiency. In the following work, we focus on the stress states of the X-shaped unit, and explore the optimization of the intersection micro structure of the junction.

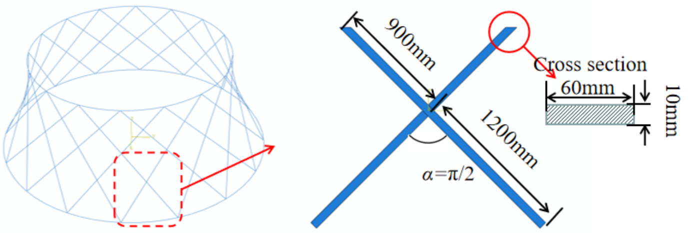

Figure 1. Abstract diagram of the bracket

3.1.2 Micro-scale layout design of the carbon fiber in the junction

In this section, based on the X-shape structure, the optimum schemes are put forward through reasonable arrangement of the carbon fiber. One common way to deal with this is to stack the unidirectional ply orthogonally, thus forming a macro local bulge in the intersection of the ribs, as shown in Fig.2a). The bulge part leads to a local buckling of the carbon fiber bundles. When the compression load is applied, bending and shearing stress will be generated at the intersection position, resulting in premature instability of the whole structure, which will greatly decrease the bearing capacity. Another way is laminating fabric to form the junction. The fabric cutting technology can avoid the local bulge of the ribs as shown in Fig.2b). In this method, two kinds of plies with different orientations are prepared by cutting and splicing process. Then, they are arranged alternately and made into the X-shaped structure by laminating and molding process. The carbon fibers are cross-oriented, it is difficult to be adjusted flexibly, only half of the carbon fibers in the rib play a full role. The material utilization ratio is low, which is not conducive to the overall performance. Thus, it is necessary to put forward a scheme that can release the overlapping phenomena in macroscale and increase carbon fiber utilization in microscale at the same time.

At present, the traditional method of preparing composite materials is to make them into unidirectional or multidirectional fiber pre-impregnating materials by laminating and molding processes. The unidirectional pre-impregnating ply thickness is between 0.125mm and 0.25 mm, which can not be flexibly adjusted. In some special structures, the thickness of the components is limited or local changes are required. Therefore, local thin-ply method is proposed[31]. The method can decrease the thickness of the ply by adjusting local arrangement of the carbon fiber, which will bring advantages to the bearing capacity due to slight changes in the microstructure, compared with the traditional methods.

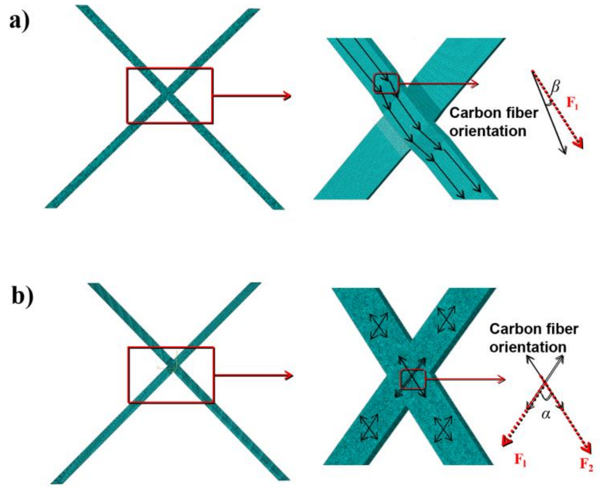

Figure 2. Schematic diagrams of two kinds of traditional X-shaped composite structure
a) Direct overlying of UD plies; b) Laminating with fabric tailoring

The local thin-ply technology is adopted in this paper, which can adjust the carbon fiber layout in the composite material, gradually increase width while reduce height of the rib components towards the intersection position. The smooth transition between the thin ply and thick ply parts is optimized to avoid stress concentration. Finally, the model is obtained, shown in Fig.3. The shape change of the rib corresponds to adjustment of the carbon fiber distribution. The carbon fibers in the middle still maintain a straight line. While, others on both sides deflect laterally to a certain extent. The extent increases with the proximity to the edges on both sides. On the whole, the orientation of most carbon fibers is in well consistent with the load transmission direction along the axial of the rib structure. Large deviation angles occur only at the edges in a very small proportion. Thus, the local thin-ply technology can retain the axial bearing advantages of carbon fiber to a large extent, and enhance the carrying capacity of the X-shaped structure.

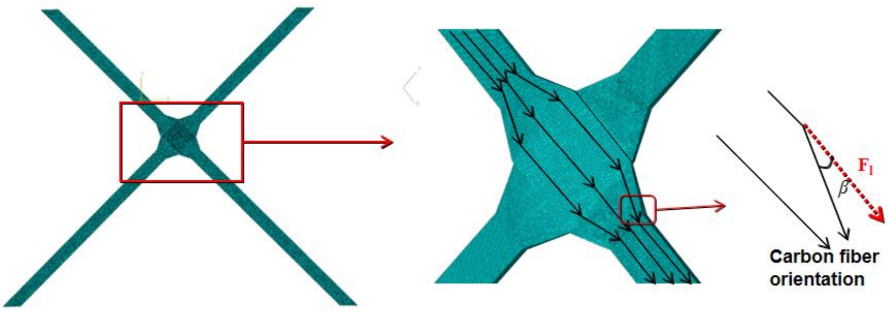

Figure 3. Schematic diagram of the X-shaped rib with local thin-ply

Similar to the traditional direct stacking method, the thin-ply method also causes a deflection of carbon fibers. However, it is in-ply bending of a small amount of carbon fiber close to the rib edges instead of the integral bending perpendicular to the ply. The different bending modes will result in performance gaps. On the one hand, under the vertical compression load, a bending moment will be generated relative to the intersection point, and the transition part of the normal/thin-ply forms a supporting structure, which is expected to improve the stability of the structure. On the other hand, at the thin-ply junction, the plies are arranged as 90-degree angle alternately, and the adjacent layers restrain each other, which greatly reduces the in-ply instability of the deflected carbon fiber at two edges of the ribs. The effectiveness of the thin-ply will be verified by comparison through finite element simulation.

3.2 Finite element simulation

For the X-shaped rib structure, the carbon fiber-matrix model in micro scale and the X-shaped rib model in macro scale are established, respectively. Swiftcomp software® is used for micro-model building, the carbon fibers evenly distribute in epoxy resin matrix, and the volume fraction is set to be 60%. For the convenience of modeling, the carbon fibers are directly bounded to the matrix, the interphases are ignored. The parameters of the epoxy resin matrix and the carbon fiber shown in table 1 are substituted to obtain the homogenized parameters of the macro composite material. Thus, a two-dimensional cross-section model is established and meshed as shown in Fig.4. The macro performance parameters obtained by homogenization calculation are shown in table 2.

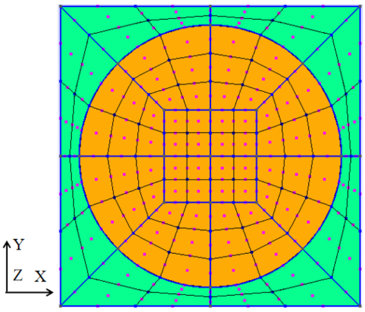

Figure 4. Micro-model and finite element model of the carbon fiber-resin matrix cell

Table 2. Homogenized parameters derived from micro-model simulation

Property	Value
E1 (Z direction, fiber direction)	139.2GPa
E2 (X direction)	6.86GPa
E3 (Y direction)	6.86GPa
G12	3.11GPa
G13	3.11GPa
G23	2.52GPa
Nu12	0.30
Nu13	0.30
Nu23	0.32

3.2.1 Comparisons of carbon fiber lamination schemes

Three kinds of macro cross-rib models, called direct stacking structure, fabric cutting structure and local thin-ply structure, respectively, are established using Abaqus software. The cross-section sizes of the ribs are the same: 60mm(W)×10mm(H), with a cross angle of 90° between them. There is a local broadening structure for the thin-ply model: the actual width of the ply is extended to 100mm towards the cross part, and the thickness is reduced accordingly as the volume conservation. The total height of the cross junction is 12mm, which is between the direct stacking one(20mm) and fabric cutting one(10mm). There is a transition area between the thin and the thick parts. The carbon fiber orientation in the area is inconsistent. In order to simplify the modeling, it is divided into nine parts, each of which is set of different fiber orientations to imitate the actual carbon fiber distribution. While, the intersecting area is laminated in an orthogonal way, namely 0 degree and 90 degree alternating $[0°/90°/0°/90°]_{25}$, the ply is shown in Fig.5. The macro models use the composite parameters in table 2 (the axial direction of the rib is set to be 0° direction). For the direct stacking and local thin-ply methods, each rib is set to be a unidirectional laminating model. While, for the fabric cutting one, carbon fibers have different orientations, the adjacent two layers are laid vertically. Shell elements are applied for the modeling. The mesh is divided by hexahedron element with the size of 5mm.

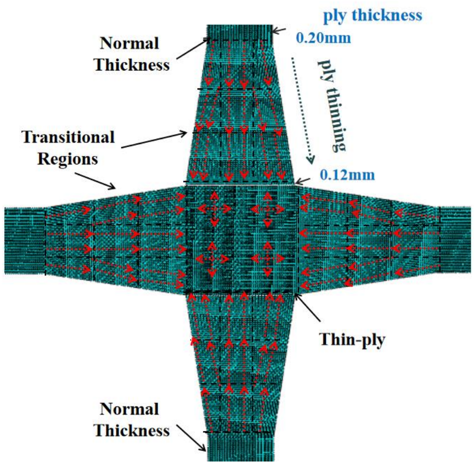

Figure 5. Orientation distribution of the carbon fiber in local thin-ply model

The bottom of the X-shaped model is fixed, a 10kN compression load is applied onto the upper end. We focus on the stress concentration state to predict and evaluate the overall bearing capacity of the structure. In the simulation process, no failure is involved. The maximum deformation is taken as the stiffness measurement, and the macro stress distribution is characterized in the form of von Mises. The local maximum principal strain in the structure is also concerned for the following dehomogenization transformation. The simulation results are shown in Fig.6.

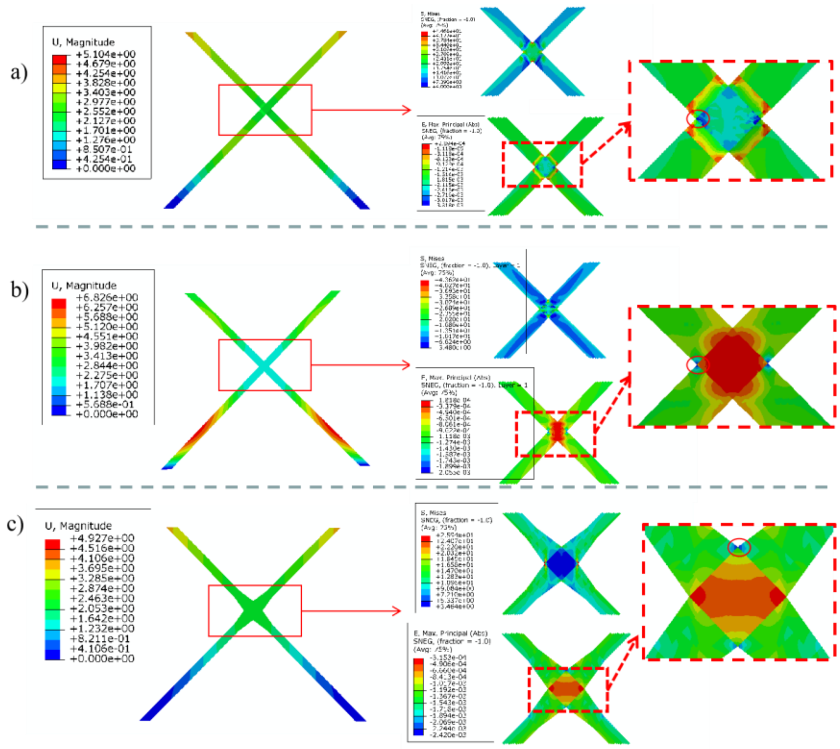

Figure 6. Simulation results of displacement, max-principal strain and shear stress distribution under loading

a) Direct stacking structure; b) Fabric cutting structure; c) Thin-ply structure

When external load reaches 10 kN, the deformations of the direct stacking structure and the local thin-ply structure are 5.10mm and 4.93mm, respectively. The maximum values both occur at the upper side along the loading direction. While, that of the fabric cutting structure appears on the lower part of the ribs instead of the upper side, which is mainly transversal deformation. The maximum value has reached 6.83mm, indicating poor stability of the fabric cutting structure. Through comparison, the local thin-ply one has exhibited the lowest deformation among the three, which corresponds to the highest overall stiffness.

In the directly stacking cross ribs, the maximum principal strain and the von Mises stress are relatively low at the ends of the ribs, both of which increase obviously at the bending position towards the junction, the maximum stress appears at the upper and lower corners of the rhombus-shaped region of the intersection, while the strain concentrate at the left and right corners. The maximum von Mises stress is 44.6MPa, and the maximum strain is 0.33 %. For the fabric cutting one, the principal strain and von Mises stress are concentrated at the same place as the former, respectively. The maximum strain is 0.21%, and the maximum stress is 43.6MPa. While the values in other positions are lower and distributed evenly. For the local thin-ply structure, the concentrate positions of stress and strain are quite different from the above. The maximum principal strain is 0.24%, which appears at the upper and lower corners of the cross area, while the max stress is 25.9MPa, lowest of the three, occupying the left and right. In contrast, the local thin-ply process has certain advantages in relieving stress and strain concentrations, which corresponds to higher structure bearing capacity and stability. This is due to the fact that most of the carbon fibers in the local thin-ply structure are in the same direction as the rib components bearing axial loads, without overall lateral bending.

In order to study the mechanical relationship between carbon fiber and matrix, and predict the failure mode in micro scale, structural dehomogenization is necessary. The data of the strain concentration area (circled in the local enlargement in Fig.6) obtained through Abaqus macro-scale simulation is extracted, which is then applied as boundary conditions for the dehomogenization simulation with Swiftcomp. The stress distribution in a single cell of carbon fiber-matrix can be obtained by reversible analytical transformation, in which the principal stress and shear stress states that we concerned are shown in Fig.7.

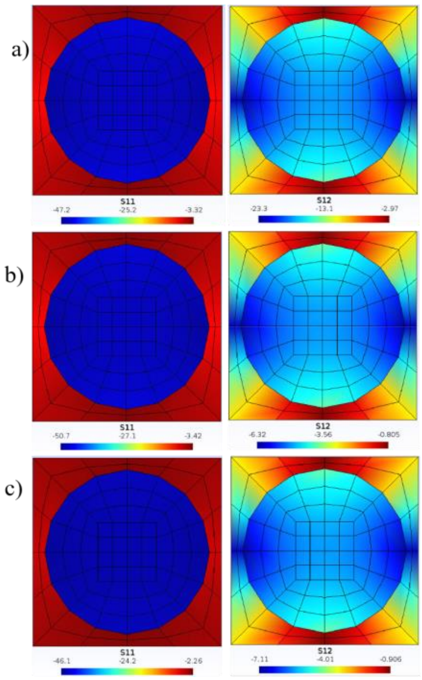

Figure 7. Local stress distribution corresponding to three models
a) Direct stacking model; b) Fabric cutting model; c) Local thin-ply model

For all the three models, the strain concentration area mainly bears compressive stress. Carbon fiber bears the main load in the composite and becomes the stress concentration area, the values are similar, varying from 46MPa to 51MPa. Which are obviously lower in the resin matrix, from 3.4MPa to 2.2MPa. The maximum shear stress of the local thin-ply model is 7.1MPa, and that of the carbon fabric cutting model is 6.3MPa, both of which are obviously lower than the direct stacking one with 23.3MPa. According to the maximum stress criterion, when composite fails there is:

$$F.I.=Max\left(\frac{\sigma_i}{X_i},\left|\frac{\sigma_{12}}{S_{12}}\right|\right) \tag{1}$$

Where: *F.I.*-failure index;
σ_i- normal stress in the i direction;
σ_{12}- shear stress;
X_i- compressive strength in the i direction;
S_{12}-in-plane shear strength.

In the formula, *F.I.*=1 is considered as the failure criterion. That is to say, when one of the normal or shear stresses in the material reaches the corresponding strength value, the material is considered to be failed. In our research, the carbon-fiber-reinforced polymer has excellent axial bearing capacity, and the above normal stress values are all far below the corresponding bearing strengths (the axial load is mainly carried by carbon fiber, and its axial compression strength can reach 1.5GPa). While, the mutli-ply structure has poor shearing capacity (S_{12} is relatively lower, around 100MPa at the interface between CF/matrix according to our previous simulation). Thus, the value of σ_{12}/S_{12} is in our research within the range of 0.063-0.233, which is much higher than those of σ_i/X_i (0.030-0.035). In the elastic deformation stage, the stress increases linearly with the load, the shear stress will reach its limitation earlier than the normal stress. In addition, the normal stress values of the three schemes are close to each other, while the shear stress exhibit large gaps, which becomes the main factor to determine the failure mode of the structure. The directly stacking structure shows the highest shear stress, in which, interface failure will first take place. As the load increases, the failure will lead to the separation between carbon fiber and the matrix. The pull-out of the carbon fiber and the initiation of cracks in the matrix near the defects will cause ultimate destruction of the macro-structure. Considering the former macro-simulation results, the stress and strain of the directly stacked structure are concentrated on the edges of the intersecting area, the local high shear stress is caused by the bulge of the cross structure, the deviation between the lateral bending ply and the loading transfer path increases the possibility of the whole structure buckling in the normal direction, the components prepared by the direct stacking process have certain disadvantages in loading capacity. While, for the shape uniformity advantage, the fabric cutting structure and the local thin-ply one own lower shear stresses, which mainly concentrated in the rib edges intersection points, due to the sudden changes in the stress bearing states (lamination direction variation and loading from unidirectional to orthogonal), it is supposed that the most likely failure mode in the cross section is in-plane bending as the instability of both edges of the ribs.

3.2.2 Optimization of width/height ratio of thin-ply structure

In the above research, the advantages and disadvantages of various schemes for the cross position of composite rib structures are compared. A particular structural parameter is selected for the local thin-ply process, the width of the thin-ply area is set as 100mm (corresponding to the ply thickness of 0.12mm). In fact, the local thin-ply technology can flexibly change the ply thickness and width according to the actual demand. The former research work confirmed that the change of width/thickness ratio will have a significant effect on the structural performance, which is further investigated in this section. Thin-ply models with different ply thicknesses are built respectively, as shown in Fig.8.

When the width of the local thin part reaches 120mm, the thickness of the ply is 0.10mm, the total height of the cross area is the same as that of the conventional rib (10mm), the local bulge is avoided. As the width of the local area decreases (such as, 100mm, 80mm and 60mm), the height of the cross position increases gradually (such as 12mm, 15mm and 20mm, respectively), an overall lateral uplift of carbon fiber occurs. When the width is reduced to 60mm, the local thin-ply structure is transformed into the direct stacked one, which is taken as an extreme case for comparison in this part. External loads of 10kN are applied on top of the models. The simulation results are shown in Fig.9. The corresponding data of stress and deformation are counted and plotted, as shown in Fig.10, where W/T is the ply width/thickness ratio of the intersection part.

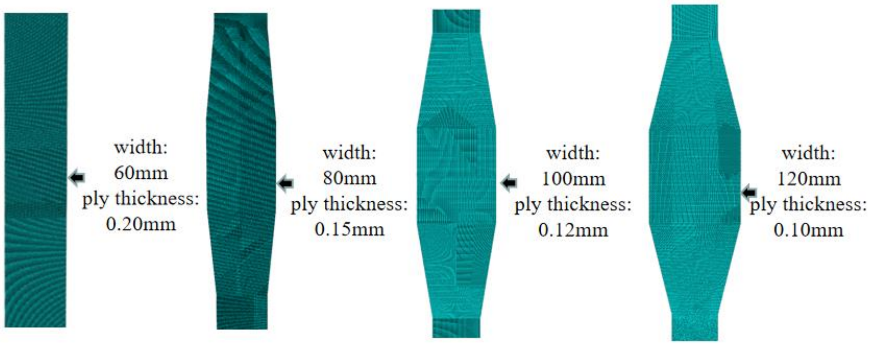

Figure 8. Schematic diagram for modeling of local thin-ply structure with different width/thickness ratio

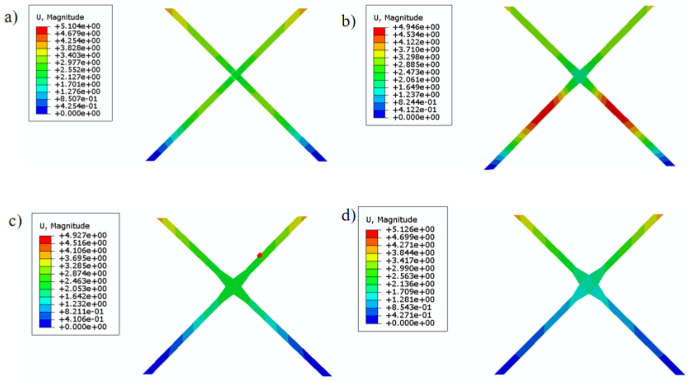

Figure 9. Deformation contour map of local laminates with different W/T ratio after loading
a) W/T=60mm/0.20mm; b) W/T=80mm/0.15mm;
c) W/T=100mm/0.12mm; d) W/T=120mm/0.10mm

As the load applied in this paper is low, the whole structure stays in the elastic deformation stage. The global deformation, local maximum von Mises stress, principal stress and shear stress increase linearly with the external load. For the external load-deformation curve, when W/T is 60mm/0.20mm, a relatively large elastic deformation occurs (5.10mm). As the ply thinning, the elastic deformation along the loading direction decreases firstly and then increases. When the W/T is 80mm/0.15mm, the deformation is only 4.55mm, that is the lowest and the maximum structure stiffness is obtained. As the W/T continues to grow till the maximum of 120mm/0.10mm, the deformation value comes back to 5.13mm.

The effect of width/thickness ratio on the distribution of stress in three different forms (max principal, shear, von Mises) is consistent. That is to say, the stress concentration is obvious and the local value is the highest when W/T is 60mm/0.2mm. The maximum stress decreases gradually with the ply thinning, which reaches the lowest when the ply width achieves 120mm. For which, in-ply bending is most likely structural instability mode, as the stress and strain concentrated on both ends of the boundary between the transition and the thin ply. The thin-ply structure shows advantages in reliving the stress concentration, improving the structural strength and the overall bearing capacity.

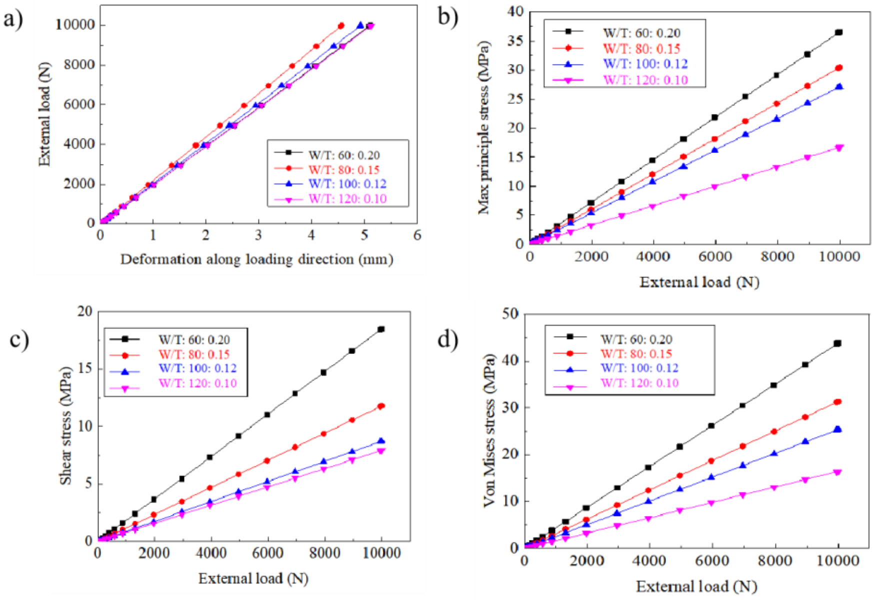

Figure 10. Variation Law of structural deformation and stress value in forms of max principal, shear and von Mises, respectively
a) Loading-deformation curves; b) Max principle stress-loading curves;
c) Shear stress-loading curves; d) Von Mises stress-loading curves

The maximum principal stress and shear stress in composite materials are the key factors to determine the bearing capacity and reliability of structures. For the X-shaped structure, the cross junction inevitably becomes the point of stress concentration. As mentioned above, the greater ply thickness of the cross-section corresponds to more pronounced local uplift by the stacking. The stress always concentrates at the mutation position of the uniform structure, the obvious uplift at the cross section can bring severe local stress concentration. Therefore, the local stress value of the W/T=60mm/0.20mm one is the maximum, which grows with the increase of the external load. When the failure strength of the material is reached, the structure destruction happens. As the decrease of local ply thickness, the uniformity of structure, the stability and bearing capacity of the components are improved. When the height of intersection is reduced to 10mm(W/T:120/0.10mm), the local uplift is completely avoided, the X-structure obtains overall uniformity, the stress distributes evenly, which corresponds to excellent structural reliability.

4. CONCLUSIONS

In this paper, an example of optimizing the X-shaped cross structure is presented. Analytic calculation and finite element simulation methods are applied. Finally, an optimized X-shaped composite structure is obtained. The following conclusions are summarized:

The multi-scale finite element simulation method is taken for the layout design of carbon fiber. The corresponding relationship between macro-performance and micro-structure is obtained by the combination of Abaqus and Swiftcomp. This paper has introduced the local thin-ply structure. The simulation results show that it can maximize the utilization of the carbon fiber bearing capacity, whose advantages are obvious comparing with the traditional direct stacking and fabric cutting ones.

The W/T ratio of local thin-ply structure has an obvious effect on the stiffness and strength. The structural stiffness depends on the orientation and deflection of carbon fiber. With the decrease of the local ply thickness, the structural stiffness first increases and then decreases, the peak is achieved at 80mm/0.15mm. While the strength and stability of the structure are increased as the thinning of the ply thickness until 120mm/0.10mm (W/T), for the improvement of structural uniformity. In the actual engineering design process, the influence of width/thickness ratio on both the structural performance and the practical requirements should be considered.

REFERENCES

[1] E.T. Thostenson, Z. Ren, and T.W. Chou, Advances in the science and technology of carbon nanotubes and their composites: a review. *Composites Science & Technology*, 61(13), 2001, pp.1899-1912.

[2] C. Barile, C. Casavola, F.D. Cillis, Mechanical comparison of new composite materials for aerospace applications - ScienceDirect. *Composites Part B: Engineering*, 162, 2019, pp. 122-128.

[3] V.V. Vasiliev, V.A. Barynin, and A.F. Razin, Anisogrid composite lattice structures- Development and aerospace applications. *Composite Structures*, 94(3), 2012, pp. 1117-1127.

[4] T.W. Chou, L. Gao, E.T. Thostenson, et al., An Assessment of the Science and Technology of Carbon Nanotube-Based Fibers and Composites. *Composite Science and Technology*, 71(1), 2010, pp. 1-19.

[5] M. Sadighi, R.C. Alderliesten, R. Benedictus, Impact resistance of fiber-metal laminates: A review. *International Journal of Impact Engineering*, 49, 2012, pp. 77-90.

[6] W. Huang, Z. Fan, W. Zhang, et al., Impulsive Response of Composite Sandwich Structure with Tetrahedral Truss Core. *Composites Science and Technology*, 176, 2019, pp. 17-28.

[7] Z. Tian, Y. Liu, L. Jiang, et al., A Review on Application of Composite Truss Bridges Composed of Hollow Structural Section Members. *Journal of Traffic and Transportation Engineering (English Edition)*, 6(01), 2019, pp. 100-114.

[8] R. Umer, Z. Barsoum, H. Jishi, et al., Analysis of the Compression Behaviour of Different Composite Lattice Designs. *Journal of Composite Materials*, 2018.

[9] L.P. Ye, P Feng, Applications and Development of Fiber Reinforced Polymer in Engineering Structures. *China Civil Eng J*, 39, 2008, pp. 24-36.

[10] P. Feng, All FRP and FRP Concrete Hybrid Components for Bridges: Experiments, Theories and Case Study. *3rd Asia-pacific Conference on FRP Instructures*, 2012.

[11] F Sewerin, On the Local Identifiability of Constituent Stress-Strain Laws for Hyperelastic Composite Materials. *Computational Mechanics*, 65, 2020, pp. 853-876.

[12] W.T. Lv.; D. Li, L. Dong, Study on Mechanical Properties of a Hierarchical Octet-Truss Structure. *Composite Structures*, 249, 2020, pp. 112640.

[13] S.J. Chen, Current Situation and Trend of Advanced Composite Materials. *Hi-Tech Fiber & Application*, 26 (6), 2001, pp. 1-5.

[14] X.B. Chen, Development of The Advanced Polymer Matrix Composite. *Aviation Maintenance &Engineering*, 3, 2001, pp. 14-16.

[15] M.S. Pfeil, A.M. Teixeira, R.C. Battista, Experimental Tests on GFRP Truss Modules for Dismountable Bridges. *Composite Structures*, 89, 2009, pp. 70-76.

[16] H.J. Chen, Analysis and Optimum Design of Composite Grid Structures. *Stanford, CA: Stanford University*, 1995.

[17] M.W. Peter, M.G. Jeff, M.H. Steven, et al., Advanced Grid Stiffened Composite Payload Shroud for The OSP Launch Vehicle. *2000 IEEE Aerospace Conference Proceedings*, 2000.

[18] P.F. Liu, Q.L. Zhao, F. Li, et al., Research on The Mechanical Properties of a Glass Fiber Reinforced Polymer-steel Combined Truss Structure. *The Scientific World Journal*, 2014, pp. 1-13.

[19] D.D. Zhang, Q.L. Zhang, Y.X. Huang, Flexural Properties of a Lightweight Hybrid FRP-aluminum Modular Space Truss Bridge System. *The Scientific World Journal*, 2014, pp. 1-13.

[20] S.J. Chen, Reunite the Material and the B7E7 Dream Airplane. *The Aviation Manufacturing Technique*, 1, 2005, pp. 34- 37.

[21] P.V. Solovyev, A.I. Gomzin, L.A. Ishbulatov, et al., Stress-Strain State Exploration of Stringer Made of Composite Materials Depending on Layers Stacking Structure. *Solid State Phenomena*, 284, 2018, pp. 71-76.

[22] B.Y. Pekmezci, A. Opurolu, Mechanical Properties of Carbon-Fabric-Reinforced High-Strength Matrices. Materials, 13(16), 2020, pp. 3508.

[23] A.V. Lopatin, E.V. Morozov, A.V. Shatov, Buckling and Vibration of Composite Lattice Elliptical Cylindrical Shells. *Proceedings of the Institution of Mechanical Engineers. Part L, Journal of Materials: Design and Application*, 233(7), 2019, pp. 1255-1266.

[24] E. Oromiehie, B.G. Prusty, P. Compston, et al., Automated Fibre Placement based Composite Structures: Review on The Defects, Impacts and Inspections Techniques. *Composite Structures*, 224, 2019, pp. 110987.

[25] C.F. Huang, M.C. He, Y.L. He, et al., Investigation of Tensile Property of Thin Ply Composite Laminate with Open-Hole Assisted by Acoustic Emission Technology. *Chinese Materials Conference. Springer, Singapore*, 2017.

[26] S.K. Bhudolia, S.C. Joshi, Y.D. Boon, Experimental and Microscopic Investigation on Mechanical Performance of Textile Spread-tow Thin Ply Composites. *Fibers and Polymers*, 20, 2019, pp. 1036-1045.

[27] L. Dong, J.P.M. Correia, N. Barth, et al., Finite Element Simulations of Temperature Distribution and of Densification of a Titanium Powder during Metal Laser Sintering. *Additive Manufacturing*, 13, 2017, pp. 37-48.

[28] B. Chopard, J.L. Falcone, P. Kunzli, et al., Multiscale Modeling: Recent Progress and Open Questions. *Multiscale & Multidiplinary Modeling Experiments & Design*, 2018.

[29] W. Yu, A Unified Theory for Constitutive Modeling of Composites. *Journal of Mechanics of Materials and Structures*, 2016, pp. 379-411.

[30] X. Liu, W. Yu, A Novel Approach to Analyze Beam-like Composite Structures Using Mechanics of Structure Genome. *Advances in Engineering Software*, 2016, pp. 238-251.

[31] S. Sangwook, Y.K. Ran, K. Kazumasa, et al., Experimental Studies of Thin-Ply Laminated Composites. *Composite Science and Technology*, 67, 2007, pp. 996-1008.

[32] P. Jadhav, Effect of Ply Drop in Aerospace Composite Structures. *Key Engineering Materials*, 847, 2020, pp. 46-51.

[33] J. Lee, C. Soutis, A Study on The Compressive Strength of Thick Carbon Fibre-Epoxy Laminates. *Composite Science and Technology*, 67, 2007, pp. 2015-2026.

[34] J. Lee, C. Soutis, Measuring the Notched Compressive Strength of Composite Laminates: Specimen Size Effects. *Composite Science and Technology*, 68, 2008, pp. 2359-2366.

[35] Technomic, Composite Materials Handbook-MIL 17, Volume 2: Polymer Matrix Composites: Materials Properties. *Crc Press*, 2000.